Friction **11**(4): 524–537 (2023)
https://doi.org/10.1007/s40544-022-0611-z
ISSN 2223-7690
CN 10-1237/TH
RESEARCH ARTICLE

One-step modification method of a superhydrophobic surface for excellent antibacterial capability

Ling LAN[1], Yue-lan DI[2,*], Hai-dou WANG[3,*], Yan-fei HUANG[2], Li-na ZHU[1], Xu-hang LI[1]

[1] *School of Engineering and Technology, China University of Geosciences (Beijing), Beijing 100083, China*

[2] *National Key Laboratory for Remanufacturing, Academy of Army Armored Forces, Beijing 100072, China*

[3] *National Engineering Research Center for Remanufacturing, Army Academy of Armored Forces, Beijing 100072, China*

Received: 18 November 2021 / Revised: 11 February 2022 / Accepted: 25 February 2022

Abstract: In this study, micro/nanostructures are fabricated on the surface of 3Cr13 stainless steel via laser etching, and a superhydrophobic coating with silver nanoparticles (AgNPs) is prepared by utilizing the reduction–adsorption properties of polydopamine (PDA). We investigate the effect of soaking time from the "one-step method" on the reduction of nano-Ag, surface wettability, and antibacterial properties. Scanning electron microscopy is performed to analyze the distribution of nano-Ag on the surface, whereas X-ray energy dispersive spectroscopy and X-ray photoelectron spectroscopy are used to analyze the crystal structures and chemical compositions of different surfaces. Samples deposited with PDA on their surface are soaked in a 1H,1H,2H,2H-perfluorodecyltriethoxysilane water–alcohol solution containing $AgNO_3$ for 3 h. Subsequently, a "one-step method" is used to prepare low-adhesion superhydrophobic surfaces containing AgNPs. As immersion progresses, more AgNPs are deposited onto the surface. Compared with the polished surface, the samples prepared via the "one-step method" show significant antibacterial properties against both gram-negative *Escherichia coli* and gram-positive *Staphylococcus aureus*. The antibacterial properties of the surface improve as immersion progresses.

Keywords: laser etching; one-step modification; polydopamine (PDA) processing; silver nanoparticles (AgNPs); antibacterial; superhydrophobic coating

1 Introduction

Bacterial adhesion and biofilm formation are potential threats in the use of medical devices. They not only cause wound infections, but also corrosion on the device surface and the reduced service life of medical devices. The interaction between bacteria and the surface of the device is key to bacterial adhesion and biofilm formation. The characteristics of the medical devices as well as the characteristics of the bacteria determine the mode of action between the bacteria and surface [1]. Therefore, researchers typically modify the surface wetting properties of materials to reduce liquid residue and destroy the living environment of bacteria to achieve antibacterial activity [2].

Inspired by the superwetting behavior of the lotus leaf surface in nature, researchers have widely adopted a superhydrophobic low-adhesion surface with a water contact angle (WCA) greater than 150° and a sliding angle (SA) less than 10° in the antibacterial field owing to its excellent self-cleaning performance [3, 4]. Superhydrophobic and low-adhesion properties are primarily contributed by the combined effect of surface micro/nanostructures and low-surface-energy materials [5]. When in contact with liquid, the air layer captured by a surface microstructure can effectively reduce the contact area between the solid and liquid. Hence, the residence time of water on the solid

* Corresponding authors: Yue-lan DI, Email: dylxinjic031@163.com; Hai-dou WANG, Email: whaidou2021@163.com

Nomenclature

AgNPs	Silver nanoparticles	PLP	Deposited PDA surface
PDA	Polydopamine	PLP-S/AgNPs	Superhydrophobic surface containing silver nanoparticles
PFDS	1H,1H,2H,2H-perfluorodecyltriethoxysilane		
E. coli	*Escherichia coli*	*N*	Number of colonies
S. aureus	*Staphylococcus aureus*	*Q*	Antibacterial adhesion rate (%)
P	Polished surface	WCA	Water contact angle (°)
PL	Etched surface	SA	Sliding angle (°)

surface is reduced significantly, which consequently reduce the adhesion of bacteria and the formation of biofilms [6, 7].

Although superhydrophobic surfaces can effectively reduce the adhesion between bacteria and solid surfaces, the fragile surface microstructure and low surface energy treatment can easily result in the loss of superhydrophobic properties and ultimately aggravate the growth of bacteria on the surface. Therefore, adding an antibacterial agent to a superhydrophobic surface is key to further improving the surface's antibacterial performance [8]. Antibacterial agents can be classified into three categories: natural antibacterial [9], synthetic antibacterial [10], and inorganic metal antibacterial [11]. Inorganic metal antibacterial agents have garnered significant attention owing to their extensive antibacterial properties and low drug resistance. They primarily include Ag, Cu, Zn, and other metals as well as their oxides [12–14]. Among them, metallic Ag exhibits the best antibacterial properties; it can destroy many types of bacteria, such as *Escherichia coli* (*E. coli*) and *Staphylococcus aureus* (*S. aureus*) [15]. In particular, silver nanoparticles (AgNPs) can release silver ions (Ag^+) into the environment, which can disrupt the permeability of bacterial cell membranes and the process of DNA replication, resulting in the leakage of bacterial cytoplasm and ultimately killing the bacteria [16].

Although superhydrophobic antibacterial surfaces containing fungicides have been reported, most require complex and laborious surface modification treatments. For example, Song et al. [17] prepared surface microstructures by continuously depositing silica nanoparticles, subjected them to amination treatment, and finally prepared superhydrophobic surfaces with synergistic antibacterial properties via perfluoroalkylsilane treatment. Qian et al. [18] first used polydopamine (PDA) and AgNPs to construct a layered micro/nanostructure on the surface of stainless steel and then treated the surface under a low surface energy with 1H,1H,2H,2H-perfluorodecanethiol. Finally, a superhydrophobic antibacterial coating was prepared. However, the surface microstructure constructed by depositing solid particles exhibited low stability and easy shedding. In addition, complex and uneconomical synthesis methods were used in those previous studies [17, 18], and the long production time involved limits their large-scale production and application. Therefore, the stability of the surface microstructure must be improved and the number of steps required for chemical modification must be reduced.

A "one-step method" is proposed herein to achieve surface bacteriostasis. The basic idea is to use the reduction–adsorption properties of dopamine to prepare a superhydrophobic surface with AgNPs on a stable grid-like microstructure surface etched using laser. The effect of the soaking time on the hydrophobicity and distribution of AgNPs is investigated. The elemental composition and structure of the sample surface are analyzed via X-ray photoelectron spectroscopy (XPS), and the "one-step" mechanism for preparing superhydrophobic surfaces containing silver nanoparticles (PLP-S/AgNPs) is investigated. The antibacterial properties of the superhydrophobic antibacterial surface against two different types of bacteria, i.e., gram-negative *E. coli* and gram-positive *S. aureus*, are evaluated experimentally. The effects of the superhydrophobicity of the surface and AgNPs on the antibacterial properties of the surface are investigated based on

several aspects. The anti-adhesion properties of the surface for both types of bacteria are analyzed using the coating counting method, and the antibacterial properties of different surfaces exposed to the environment are evaluated using the turbidity method. Finally, the effects of the different surfaces on the formation of *E. coli* biofilms are analyzed via laser confocal microscopy. Compared with the conventional preparation of superhydrophobic antibacterial surfaces, the one-step immersion modification treatment method proposed herein allows antibacterial agents to be deposited simultaneously and the surface energy to be reduced. Consequently, the surface modification time is reduced, and the utilization rate of the material is improved.

2 Experimental materials and methods

The experimental process is shown in Fig. 1. First, the sample is polished, laser-etched, PDA adsorbed, and immersed in a 1H,1H,2H,2H-perfluorodecyltriethoxysilane (PFDS) water–alcohol solution containing $AgNO_3$ sequentially to prepare a superhydrophobic surface with AgNPs. Second, the scanning electron microscopy (SEM) is performed to observe the surface morphologies of the samples at each stage, measure the surface wettability, and determine the atomic percentage and elemental chemical structure. Finally, antibacterial adhesion test and live/dead bacteria control tests are performed to compare the horizontal antibacterial properties of each sample surface.

2.1 Materials

As a substrate for the experiment, 3Cr13 stainless steel, which is typically used to manufacture medical equipment, was selected and cut into individual pieces measuring 10 mm × 10 mm × 1 mm. Tris (hydroxymethyl) aminomethane was purchased from Beijing Twbio Technology Co., Ltd.; dopamine hydrochloride was purchased from Shanghai Minrel Chemical Technology Co., Ltd.; and silver nitrate ($AgNO_3$) and hydrochloric acid were purchased from Beijing Lange Chemical Products Co., Ltd. Anhydrous ethanol and acetone were purchased from Beijing Tongguang Fine Chemical Co., Ltd., whereas PFDS and deionized water were purchased from Aladdin Reagent (Shanghai) Co., Ltd. All chemicals were used as received without further purification. *E. coli* (CFT 073) and *S. aureus* (ATCC 29213) were obtained from the Chinese Center for Disease Control and Prevention.

2.2 Preparation of superhydrophobic/antibacterial surface

The 3Cr13 stainless steel samples were polished with sandpaper to 2000 grains, ultrasonically cleaned with acetone, absolute ethanol, and deionized water for 3 min, and then dried at room temperature. In the experiment, a nanosecond fiber laser was used to prepare an isotropic grid-like microstructure through orthogonal line scanning. The processing parameters are listed in Table 1. The etched samples were placed in an ultrasonic cleaning machine, washed with acetone, absolute ethanol, and deionized water for 10 min

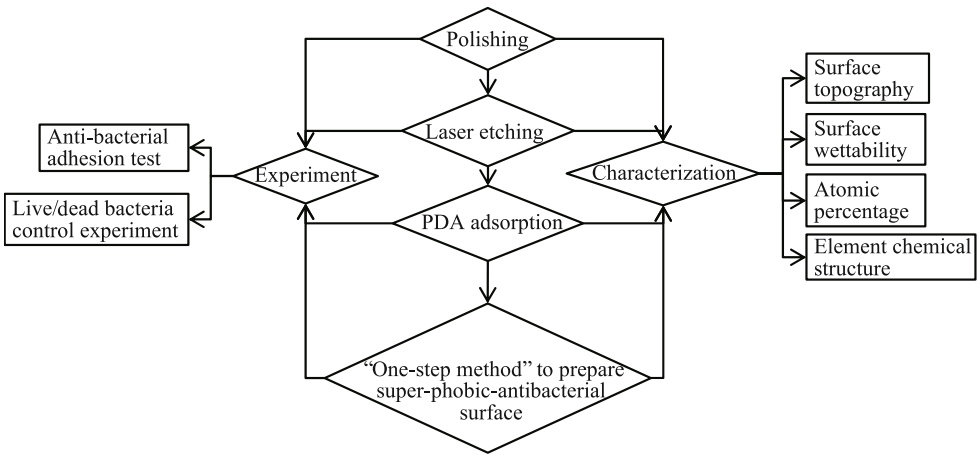

Fig. 1 Flow chart of experiment.

Table 1 Laser etching parameters.

Processing parameter	Processing power (W)	Spot diameter (μm)	Etching speed (mm/s)	Etching time (time)	Processing frequency (kHz)
Amount	20	50	1,000	5	20

each, and then dried at room temperature. First, the sample was immersed in Tris–HCl buffer (10 mM, pH=8.5) containing dopamine hydrochloride (2 mg/mL) and allowed to stand for 24 h. Subsequently, the sample was removed and ultrasonically cleaned with deionized water for 3 min. Second, the sample was immersed in a PFDS water–alcohol solution (5 mmol/L, *V*(water):*V*(alcohol) = 2:8) containing $AgNO_3$ (5 mg/mL) for 3 h (PLP-S/AgNPs$_{3h}$) and 12 h (PLP-S/AgNPs$_{12h}$). Finally, the sample was ultrasonically cleaned with deionized water for 1 min, solidified at a constant temperature of 150 °C for 1 h, and allowed to cool naturally for later use.

The sample surfaces used during the experiment were named the polished surface (P), etched surface (PL), deposited PDA surface (PLP), and PLP-S/AgNPs.

2.3 Surface state characterization

The microscopic morphologies of the different surfaces were observed using field-emission SEM (Zeiss Gemini300, Germany). Energy-dispersive spectroscopy and XPS were used to analyze the chemical compositions and structures of the different surfaces. The samples were cured in a constant-temperature blast-drying oven (DH-101-2BS, Tianjin Central Experiment Furnace Co., Ltd., China). The wettability of the samples was measured using an optical contact angle measuring instrument (Harke SPCA-X3, China). At room temperature, a water droplet of 5 μL was deposited to measure the WCA of the sample surface, and a water droplet of 10 μL was deposited to measure the SA of the sample surface using the inclined plate method. The SA is defined as the inclination angle of the inclined plate when a water droplet of 10 μL begins to roll on the inclined plate.

2.4 Antibacterial adhesion test

Strains of gram-negative *E. coli* and gram-positive *S. aureus* were used in the experiments to investigate the anti-adhesion properties of the material surface for different microorganisms. Prior to the experiment, all samples were sterilized with 75% alcohol. The experimental surface was placed in a brain heart infusion (BHI) medium in a constant temperature incubator to assess the sterilization of the surface. A single colony of bacteria was selected using an inoculation loop and placed in the BHI broth in a constant-temperature rotating bed for certain duration. Cultured bacterial suspensions were centrifuged for 5 min. After removing the supernatant, the cells were resuspended in sterile phosphate buffered saline (PBS) until the optical density at 600 nm (OD 600) of the bacterial suspension was 0.3.

The sample was placed in a PBS suspension containing bacteria for 5 min, after which the bacterial suspension was aspirated. The surface of each sample was cleaned using sterile PBS solution. Subsequently, the sample was transferred to a centrifuge tube containing sterile PBS solution and ultrasonically shaken to elute the bacteria attached to the surface of the sample. The washed bacterial solution was diluted 10 times, and 100 μL of each bacterial solution was applied evenly to the BHI solid medium. Subsequently, the solution was incubated at a constant temperature, and the number of colonies (*N*) was counted. After ultrasonic cleaning, the sample was washed twice with sterile PBS solution, stained with 1% crystal violet solution for 30 min, and washed twice with sterile PBS solution. The surface-cleaning efficacy was observed using a confocal laser scanning microscope (Zeiss LSM710, Germany) [19].

2.5 Live/dead bacteria control experiment

To further investigate the antibacterial activity on the surface of the material and its ability to inhibit biofilm formation, experiments were performed using gram-negative *E. coli*. Furthermore, alcohol sterilization and culture plates were used to determine the sterilization of the surface. A single colony of *E. coli* was selected from an inoculation loop to be grown in a BHI broth medium; subsequently, it was placed on a constant-temperature rotating bed until the

OD 600 reached 0.3. The sample was placed in 2 mL of 20-fold diluted bacterial solution and incubated for 16 h at a constant temperature. After incubation, the absorbance of the bacterial solution was measured using a ultraviolet-visible spectrophotometer (Varian CARI-50, USA) at a wavelength of 600 nm (using the sterilized BHI culture solution as a reference), and the turbidimetric method was used to evaluate the antibacterial performance of the material. A calcein-acetyl methoxy methyl ester (AM)/propidium iodide (PI) live/dead bacteria double-color staining Kit (Beijing Solarbio Science & Technology Co., Ltd., China) was used to distinguish live/dead cells via *in situ* fluorescent staining to evaluate the antibacterial activity of the material surface [20]. The live/dead bacterial stain was configured based on the kit instructions and soaked in the stain for 20 min. Subsequently, five locations on the sample surface were observed randomly using a confocal laser scanning microscope (Zeiss LSM710, Germany) (live and dead bacterial cells were stained with green and red fluorescence, respectively). The ImageJ software (National Institutes of Health, Bethesda, USA) was used to calculate area coated with *E. coli* on the sample surface.

3 Results

3.1 Surface morphology and surface wettability

The surface micromorphologies of the PL, PLP, PLP-S/AgNPs$_{3h}$, and PLP-S/AgNPs$_{12h}$ samples are shown in Fig. 2. After laser etching, a stable grid-like microstructure is formed on the surface (Figs. 2(a1) and 2(b1)), and further magnification shows numerous nanoparticles attached to the surface (Fig. 2(a2)). Soaking the samples in dopamine solution did not significantly change their microscopic surface morphologies (Fig. 2(b2)). After the sample was soaked in a PFDS water–alcohol solution containing $AgNO_3$ for 3 h, the number of discrete AgNPs on its surface was reduced significantly (Fig. 2(c2)). As immersion progressed, the surface reduction of the AgNPs increased gradually. At 12 h of immersion, a uniform and dense layer of AgNPs was successfully formed on the surface (Fig. 2(d2)). The diameter of the AgNPs was between 10 and 50 nm.

Photographs of the surface wettability and water drop contact of P, PL, PLP, PLP-S/AgNPs$_{3h}$, and PLP-S/AgNPs$_{12h}$ are shown in Fig. 3. The WCA of the polished surface (P) was 80.79°, at which the droplet did not slide. After laser etching was performed, the static contact angle reduced to 33.42°. After PDA treatment, the contact angle of the surface further decreased to 21.26°. After the sample was soaked in a PFDS water–alcohol solution containing $AgNO_3$, the surface transformed promptly into a superhydrophobic and low-adhesion state. As immersion progressed, both the WCA and SA increased gradually. At 12 h of immersion, the WCA and SA of the sample surface were 160.20° and 7.2°, respectively.

Table 2 lists the atomic percentage ratios of the main elements constituting the surfaces of the different samples. Figure 4 shows the atomic percentage curves of four of the elements, i.e., C, O, F, and Ag, in each preparation stage. The atomic percentage of O increased significantly from 2.21% to 21.97% after laser etching. This is because the metal elements on the surface of stainless steel underwent oxidation reactions during the etching process in an atmospheric

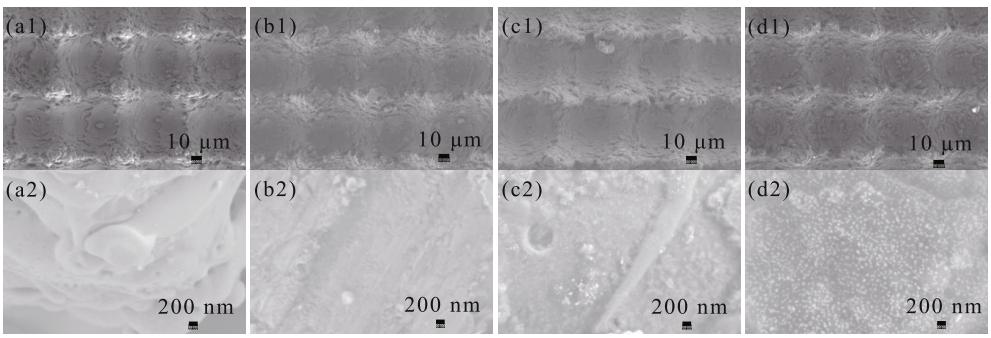

Fig. 2 Scanning electron micrography images of the samples: (a1, a2) PL, (b1, b2) PLP, (c1, c2) PLP-S/AgNPs$_{3h}$, and (d1, d2) PLP-S/AgNPs$_{12h}$.

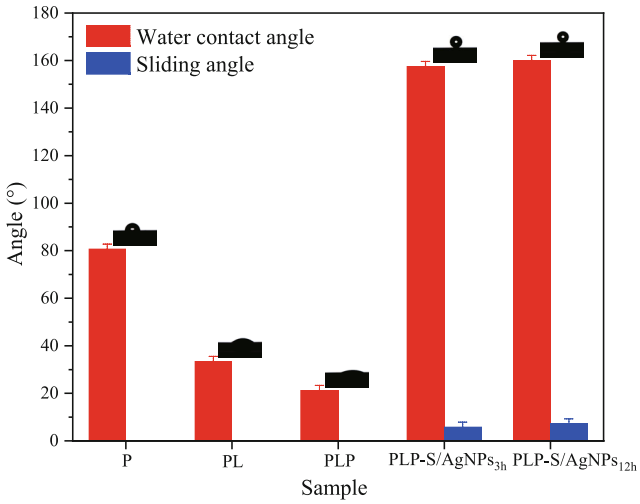

Fig. 3 Photographs of surface wettability and water droplet contact of the samples at various stages.

Table 2 Atomic content percentage of main elements on the sample surface at each stage. (Unit: at%)

Sample	C	N	O	F	Cr	Fe	Si	Ag
P	12.88	0	2.21	0	13.21	71.43	0.27	0
PL	12.58	0	21.97	0	3.5	60.97	0.98	0
PLP	48.64	0.79	20.73	0	0	29.5	0.34	0
PLP-S/AgNPs$_{3h}$	37.31	0	16.31	0.62	1.52	43.11	0.86	0.27
PLP-S/AgNPs$_{12h}$	42.53	0	14.83	11.8	0.21	28.68	1.29	0.67

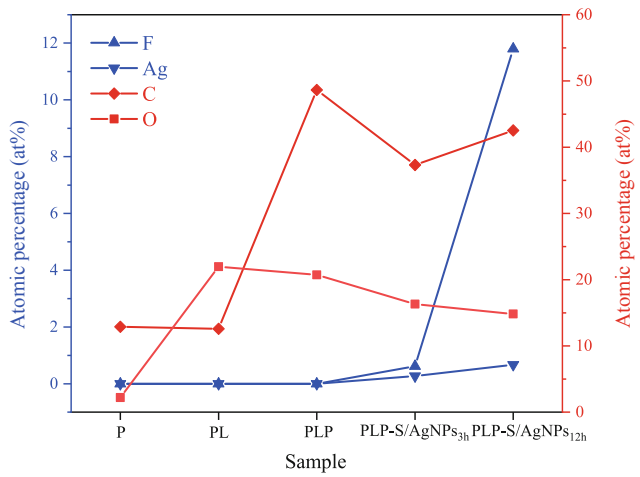

Fig. 4 Atomic percentage curves of C, O, F, and Ag at each stage.

environment. After the sample was soaked in dopamine solution, the atomic percentage of C increased by 3.86 times. Meanwhile, the atomic percentage of N was 0.79%, which is attributable to the imine group in PDA [21]. After the treated sample was soaked in a PFDS water–alcohol solution containing $AgNO_3$ for 3 h, Ag and F appeared on the surface. In addition, the atomic percentage of Si increased from 0.34% to 0.86%. The increase in the atomic percentages of F, Si, and Ag indicates that the surface had successfully adsorbed PFDS molecules while reducing the number of AgNPs. The atomic percentages of F and Ag increased with the immersion time. Furthermore, the atomic percentages of F and Ag on the surface of the PLP-S/AgNPs$_{12h}$ increased to 11.8% and 0.67%, respectively. The disappearance of N requires further investigation; however, the change in its amount does not significantly affect the experimental result. Therefore, it is not discussed in detail herein.

The chemical compositions of F and Ag on the surface of the obtained PLP-S/AgNPs$_{12h}$ were characterized via XPS based on a spot diameter of 100 μm. The high-resolution spectra of F and Ag are shown in Fig. 5. After the sample was immersed in a PFDS water–alcohol solution containing $AgNO_3$ for 12 h, only C–F groups were observed in the high-resolution energy spectrum of F 1s (Fig. 5(a)), with a binding energy of 687.2 eV. This shows that the fluorosilyl group in the PFDS molecule did not decompose during dopamine treatment. It is noteworthy that two peaks with binding energies of 373.6 and 367.7 eV appeared in the high-resolution energy spectrum of Ag 3d (Fig. 5(b)), which correspond to Ag 3d5/2 and Ag 3d3/2, respectively. The appearance of Ag 3d indicates the formation of elemental AgNPs on PLP. Results of Ag analysis show that the reduced AgNPs were not oxidized and only adhered to the surface of the sample in the form of simple Ag. In addition, the Ag on the surface did not react with F, and no toxic AgF was produced.

3.2 Bacterial adhesion test results

First, we examined the sample for contamination prior to the experiment by placing it in a culture medium and then incubating it at a constant temperature. Figure 6 shows the P, PL, PLP, PLP-S/AgNPs$_{3h}$, and PLP-S/AgNPs$_{12h}$ samples and culture medium after the contamination test. Colony formation was not indicated on the sticky surface (in the white box), which indicates the absence of bacterial residue on

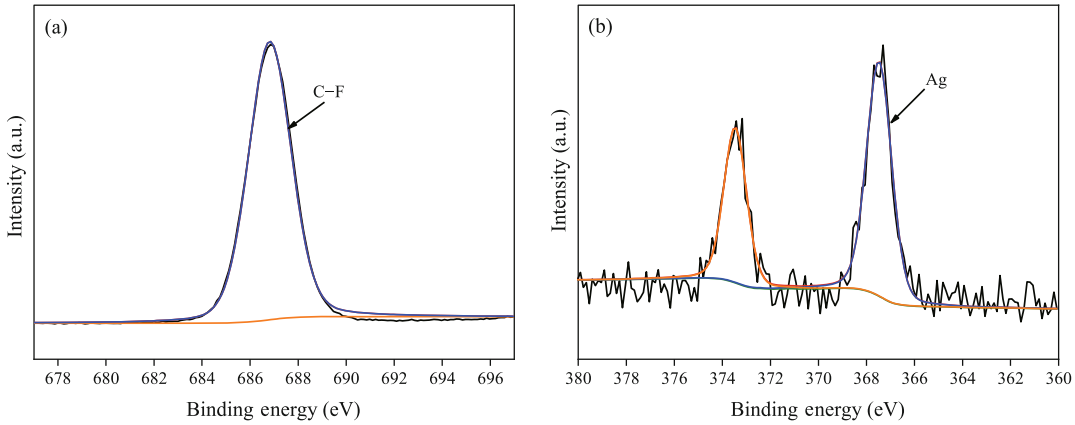

Fig. 5 High-resolution spectra of (a) F and (b) Ag.

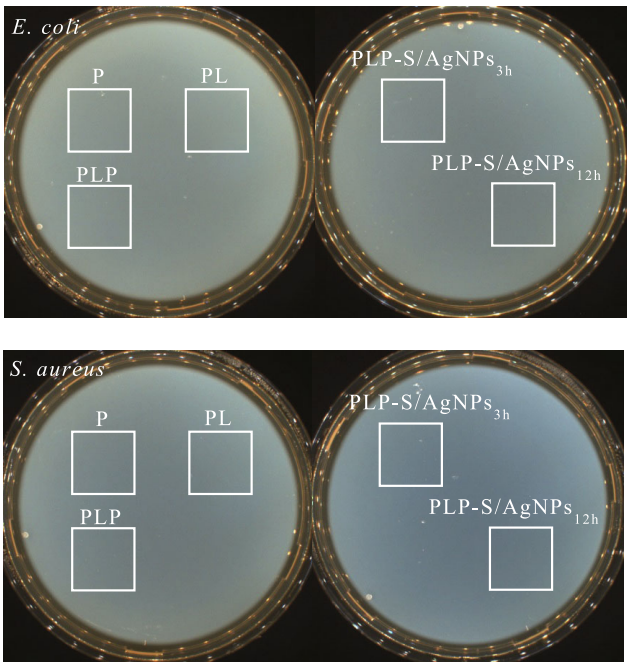

Fig. 6 Pictures of surfaces of different samples on sticky culture medium.

the surface of the sample after alcohol sterilization, as well as the non-contamination of the sample.

The antibacterial adhesion performance of the surfaces of different samples was verified via a coating counting experiment. Figure 7 shows the photographs of two types of bacteria diluted 10-fold. Compared with the polished samples, *E. coli* and *S. aureus* were more densely distributed on the sample surface after laser etching and dopamine treatment. This indicates that more bacteria were washed off from the surface, further proving that bacteria are more likely to adhere to hydrophilic surfaces. It is noteworthy that *E. coli* and *S. aureus* on the superhydrophobic antibacterial surface were sparsely distributed on the culture medium, and the N of the two bacteria decreased as immersion progressed. This shows that the superhydrophobic antibacterial surface can effectively inhibit the adhesion of *E. coli* and *S. aureus*.

To quantify the antibacterial adhesion performance of the superhydrophobic antibacterial surface more accurately, the N values of *E. coli* and *S. aureus* on the culture plate under different conditions were determined using the streaking partition method (Fig. 8). The antibacterial adhesion rate Q of the PLP-S/AgNPs sample was calculated. The formula used is as follows:

$$Q = \frac{N_{\mathrm{P}} - N_{\mathrm{PLP\text{-}S/AgNPs}}}{N_{\mathrm{P}}} \times 100\% \tag{1}$$

Where N_{P} and $N_{\mathrm{PLP\text{-}S/AgNPs}}$ represent the numbers of colonies on the surfaces of the P and PLP-S/AgNPs samples, respectively.

After being immersed in PFDS water–alcohol solution containing $AgNO_3$ for 12 h, the sample exhibited the best antibacterial adhesion performance. Its anti-adhesion rates against *E. coli* and *S. aureus* were 86.3% and 91.7%, respectively.

The fluorescence luminescence of different surfaces was observed using laser confocal microscopy to determine the presence of bacterial residue on the surface of the samples after ultrasonic cleaning. As presented in Fig. 9, bacterial luminescence is not shown on the surface of the sample after washing, which implies the removal of all bacteria that adhered to the surface of the different samples, and

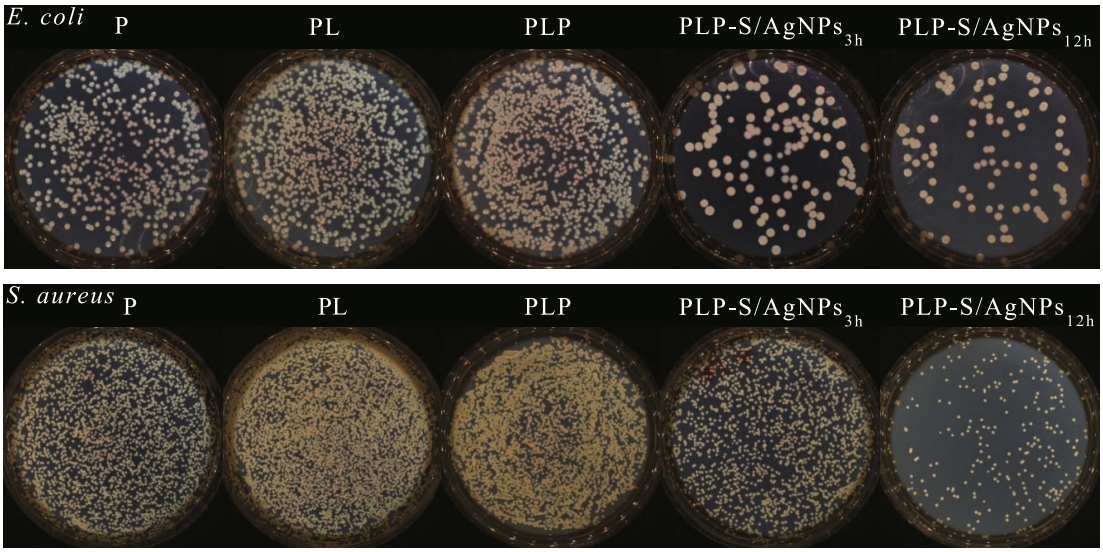

Fig. 7 Colony pictures of *E. coli*/*S. aureus* (diluted 10 times).

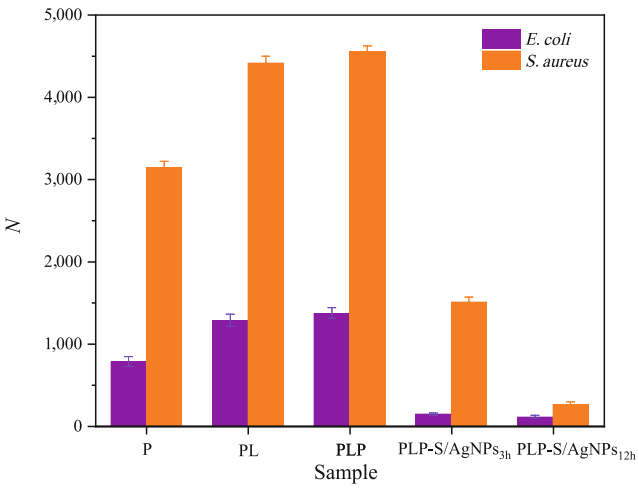

Fig. 8 *N* on surface of different samples.

the absence of residual bacteria on the surface of the sample. This further proves the accuracy of the coating plate counting assay.

3.3 Live/dead bacteria staining test results

To examine whether the samples were contaminated prior to the experiment, the alcohol-sterilized samples and the culture medium were adhered together and placed in a constant temperature incubator for 24 h. Figure 10 shows the P, PL, PLP, PLP-S/AgNPs$_{3h}$, and PLP-S/AgNPs$_{12h}$ samples and the culture medium after incubation at a constant temperature. No colony formation was indicated in the sticky area (white box), which implies the absence of bacterial residue on the surface of the sample after alcohol sterilization, as well as the non-contamination of the sample surface during the staining experiment with live/dead bacteria.

Figure 11 shows the OD 600 value of the bacterial solution after that the different samples were incubated with the bacterial solution for 16 h. As shown in Fig. 11, relative to the polished sample, the optical density (OD) value of the bacterial solution after laser etching and further treatment with dopamine remain unchanged. However, the OD 600 of *E. coli* bacteria liquid reduced by approximately 0.3 after the superhydrophobic antibacterial sample was soaked. Among them, the OD value of the bacterial solution of the sample after soaking in the PFDS water–alcohol solution containing $AgNO_3$ for 12 h is the lowest, at approximately 0.739. This indicates that PLP-S/AgNPs can effectively inhibit the growth and reproduction of bacteria.

To further analyze bacterial adhesion and biofilm formation on the surface of the different samples, *E. coli* was observed via laser confocal microscopy (Fig. 12). As shown in Fig. 12, a significant amount of *E. coli* adhered to the surface of the polished sample, and an extensive biofilm was formed on the surface. After laser etching and further treatment with dopamine, a significant amount of live *E. coli* and biofilms distributed widely on the microstructures. It is noteworthy that the amount of *E. coli* adhering to the superhydrophobic antibacterial surface reduced

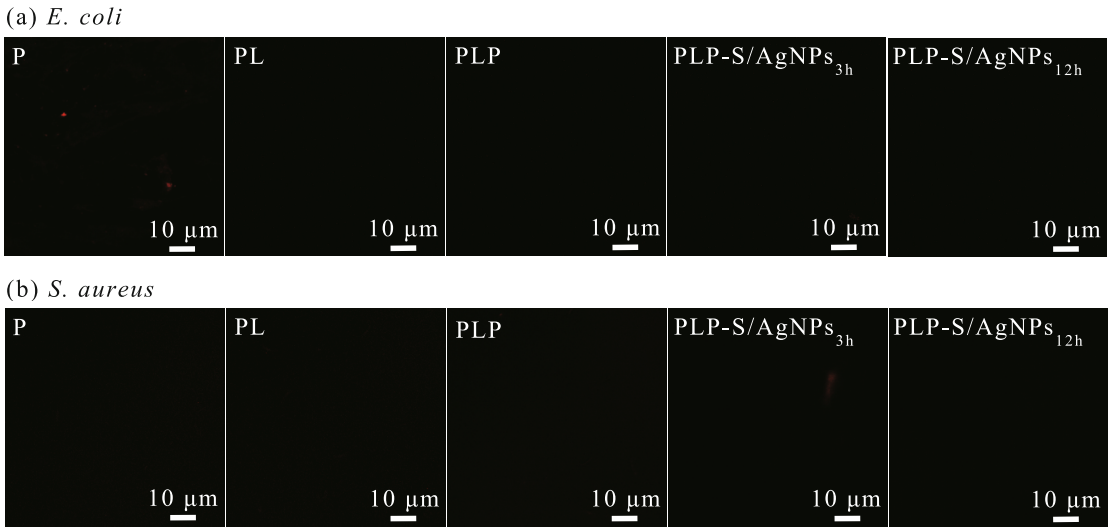

Fig. 9 Laser confocal observation photographs of different sample surfaces after cleaning.

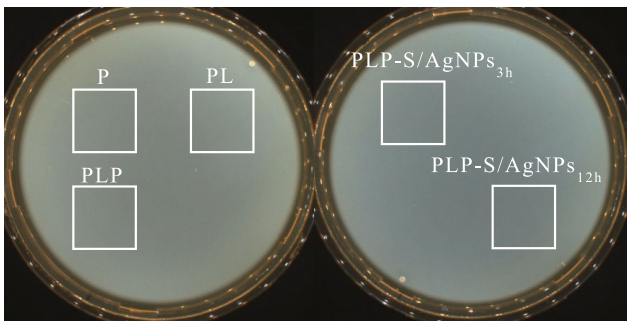

Fig. 10 Pictures of surfaces of different samples on sticky culture medium.

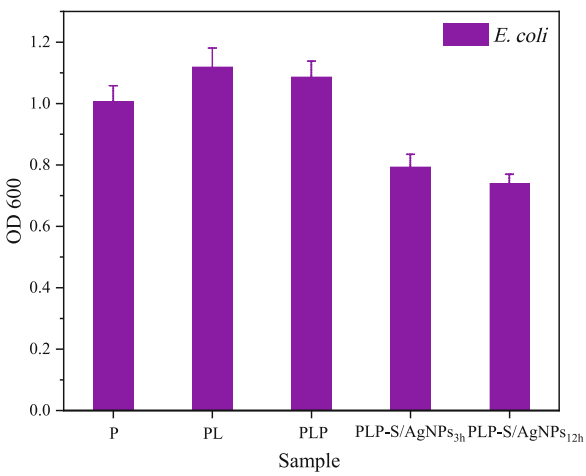

Fig. 11 OD 600 of the bacterial solution after the different samples were soaked.

significantly, and only a slight amount of *E. coli* adhered to the protrusions of the microstructure. In addition, almost no live/dead *E. coli* was observed on the surface of the PLP-S/AgNPs$_{12h}$ samples. The fluorescence intensity of live/dead *E. coli* on the surface, as shown in Fig. 13, reflects the antibacterial properties of the surface. Compared with the polished sample, the sample surface after laser etching and further treatment with dopamine demonstrates higher fluorescence intensity. This shows that hydrophilic surfaces promote bacterial adhesion and biofilm formation.

The fluorescence intensity of the surface of the PLP-S/AgNPs decreased significantly as immersion progressed. The fluorescence intensity of live/dead *E. coli* on the surface of PLP-S/AgNPs$_{12h}$ was the lowest, and the fluorescence intensities of live and dead bacteria on the surface of PLP-S/AgNPs$_{12h}$ were 2.11% and 2.96% of those on the polished samples, respectively. In addition, the proportion of dead bacteria in the PLP-S/AgNPs increased, indicating the ability of the surface in destroying bacteria. This proves that the superhydrophobic antibacterial surface can effectively inhibit the growth of bacteria and the formation of biofilms.

4 Discussion

4.1 Mechanism of "one step" preparation of PLP-S/AgNPs

Although most bacteria can be repelled by superhydrophobic surfaces, some bacteria may still

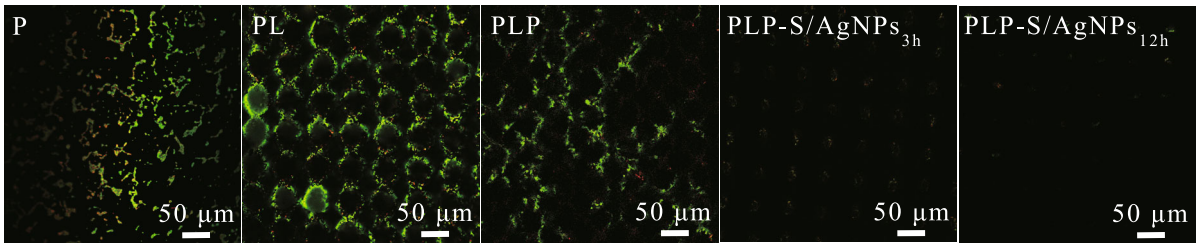

Fig. 12 Confocal laser confocal microscope observation of live/dead *E. coli* on surface of different samples.

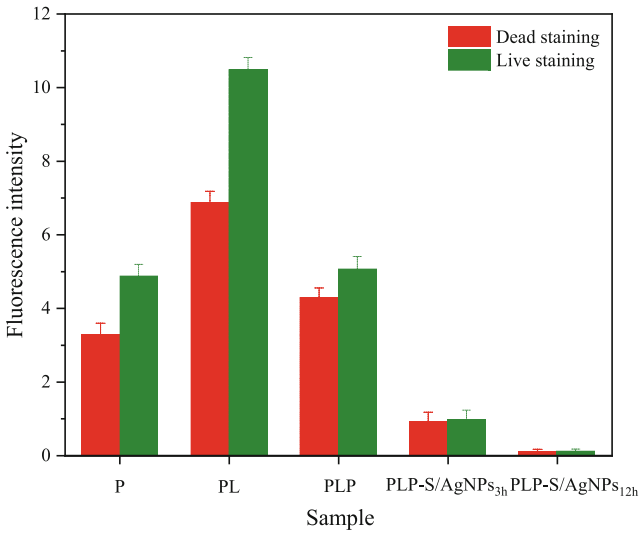

Fig. 13 Live/dead fluorescence intensity of *E. coli* on surface of different samples.

remain on solid surfaces, which inevitably results in the formation of biofilms. The introduction of antibacterial agents on superhydrophobic surfaces can significantly improve their antibacterial properties. Figure 14 shows a schematic illustration of the "one-step" preparation of superhydrophobic and antibacterial surfaces. The stable periodic grid-like microstructure is formed via laser etching. It can increase the roughness of the sample and endow it with superhydrophobic properties. Meanwhile, increasing the specific surface area allows dopamine molecules to adhere easily to the surface of the sample. The sample is further immersed in dopamine hydrochloride solution and left to stand such that the dopamine is oxidized to 5,6-dihydroxyindole, and spontaneous polymerization occurs on the surface of the stainless steel to generate PDA molecules [22]. PDA molecules easily adhere to the surface of various materials through noncovalent bonding effects, such as metal coordination or chelation, hydrogen bonding, π–π stacking, and quinhydrone charge transfer complexes [23, 24]. In addition, the catechol groups in PDA facilitates the hydroxylation of the sample surface, which consequently allows PFDS molecules to be adsorbed easily on the surface and reduces the time for surface energy reduction treatment.

$AgNO_3$ is a salt that is insoluble in ethanol. Meanwhile, the fluorosilyl group in the PFDS molecule exhibits strong hydrophobic properties and is insoluble in water. Therefore, when $AgNO_3$ is added to a water–alcohol solution containing PFDS, the two solvents will not react, which allows the one-step reduction of AgNPs and the preparation of superhydrophobic surfaces by soaking the sample with attached PDA molecules in a PFDS water–alcohol solution containing $AgNO_3$. The catechol group in the PDA molecule exhibits weak reducibility and can release electrons when oxidized to the corresponding quinone group, thereby triggering the *in situ* reduction of Ag^+ in the mixed solution to AgNPs [25, 26]. Simultaneously, the hydroxyl groups in PDA can adsorb PFDS molecules in the mixed solution, thereby reducing the surface energy of the sample surface. The reduction–adsorption properties of the PDA molecules can reduce the surface energy of the sample while reducing the AgNPs on the laser-textured surface; hence, a superhydrophobic surface with AgNPs is prepared in one step.

4.2 Analysis of antibacterial performance

The increase in surface roughness of hydrophilic materials reduces the WCA. Stainless steel is a hydrophilic material. In the experiment, the surface roughness of the laser-etched samples increased, and their specific microstructure reduced the surface WCA. Meanwhile, the introduction of hydrophilic groups also reduces the surface WCA [27]. Dopamine

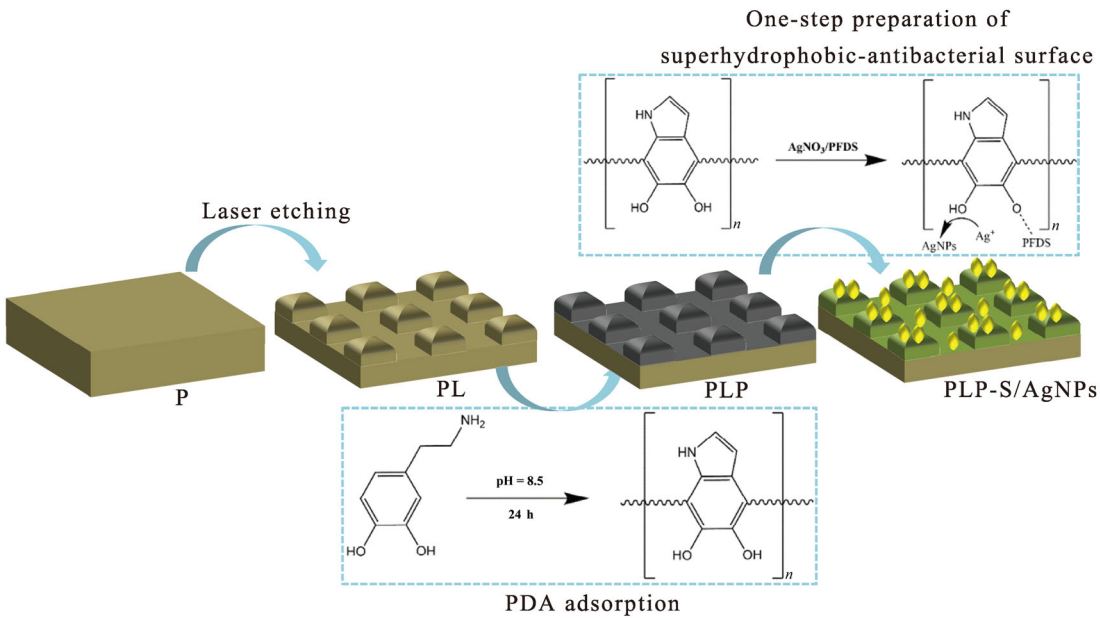

Fig. 14 Schematic diagram of "one-step" preparation of superhydrophobic/antibacterial surfaces.

contains hydrophilic catechol and amine groups; after the samples were further treated with dopamine, they exhibited a smaller contact angle. Compared with the polished samples, the laser-etched samples and dopamine-treated samples are more hydrophilic, which renders it easier for bacteria to adhere and grow on the surface of the sample, consequently resulting in the formation of a wider biofilm on the surface. The reasons for this phenomenon can be explained as follows: First, according to the Wenzel wetting theory [28],

$$\cos\theta_{\mathrm{w}} = r\cos\theta \tag{2}$$

The actual contact angle θ_{w} of the liquid is proportional to the roughness factor r and intrinsic contact angle θ. Here, r is the ratio of the actual surface area to the solid–liquid contact surface area. For hydrophilic materials, a smaller contact angle corresponds to a larger solid–liquid contact area. When the bacterial liquid is in contact with the sample surface, the larger solid–liquid contact area causes more bacteria to adhere to the sample surface. Second, the surface energy of the hydrophilic surface is higher, which improves the adsorption capacity of water and hence increases the adhesion of bacteria to the surface (Fig. 15(a)).

Figure 15(b) shows a schematic diagram of the anti-adhesion and sterilization of the superhydrophobic antibacterial surface. Its antibacterial effect originates primarily from two aspects. First, the PLP-S/AgNPs samples exhibit superhydrophobic and low adhesion properties, which conform to the Cassie–Baxter theory [29]. The Cassie–Baxter theory states that a liquid is in contact with a solid surface in the form of a solid–liquid–gas three-phase composite. The introduction of an air layer not only reduces the solid–liquid contact area, but also reduces the adhesion of the solid to the liquid such that the liquid can roll on the solid surface more easily. When the bacterial liquid is in contact with the superhydrophobic/antibacterial surface, the microstructure and PFDS molecules cooperate synergistically to form a stable air layer on the surface. Compared with the polished surface (P), the air layer significantly reduced the solid–liquid contact area, thereby reducing the adhesion of bacteria on the stainless steel surface. By contrast, the AgNPs on the surface of the PLP-S/AgNPs sample exhibit strong bactericidal properties, which can further kill the bacteria adhering to the surface of the sample. Its antibacterial activity is owing to the synergy between the release of dissolved Ag^+ and the specific effects of nanoparticles [30, 31]. When the bacterial liquid was placed in contact with the surface of the PLP-S/AgNPs sample, the AgNPs adhering to the surface released Ag^+ into the bacterial

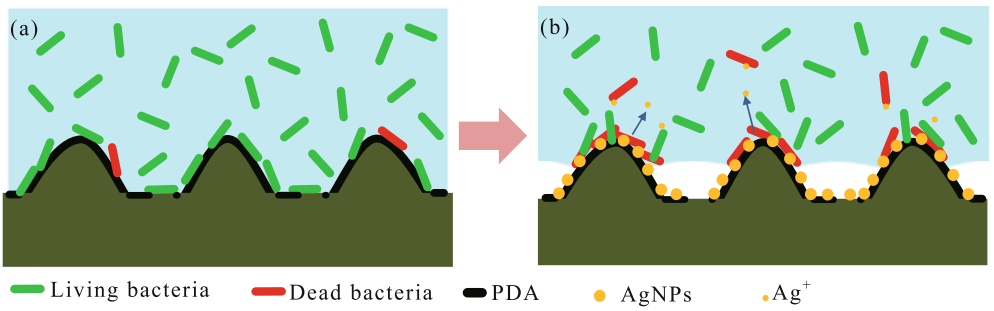

Fig. 15 Schematic diagrams showing (a) effect of bacterial adhesion on hydrophilic surfaces and (b) anti-adhesion bactericidal effects on superhydrophobic antibacterial surfaces.

liquid [25]. Ag^+ has been shown to bind to proteins in the cell membrane and form stable bonds, resulting in protein inactivation [32]. In addition, Ag^+ can form a complex with nucleic acids, thus ultimately preventing cell division and reproduction [33]. By prolonging the soaking time of the "one-step method," the number of surface-reduced adsorbed AgNPs can be increased and hence the antibacterial properties of the surface improved.

The antibacterial properties of the material surface are associated closely with the low adhesion of the superhydrophobic surface and the Ag^+ released by the AgNPs. By combining rough microstructures and low surface energy modifiers, a non-wetting superhydrophobic surface can be constructed between the solid surface and bacterial culture medium. The non-wetting surface formed by the air film in the microstructure can effectively prevent bacterial adhesion and biofilm formation. Meanwhile, superhydrophobic surfaces can control the release of AgNPs, which enables the surface to exhibit better antibacterial ability for a longer duration [18].

5 Conclusions

A superthin antibacterial surface with antibacterial adhesion and bactericidal properties was developed to prevent the adhesion of microorganisms to the surface. In this study, using the reduction–adsorption properties of dopamine, a self-assembly method was used to prepare a superhydrophobic antibacterial coating containing AgNPs on the surface of laser-textured stainless steel using a "one-step method." As immersion progressed, more AgNPs were adsorbed on the surface of the PLP-S/AgNPs. Surface antibacterial experiments were performed using gram-negative *E. coli* and gram-positive *S. aureus*. The experimental results showed that the PLP-S/AgNPs samples exhibited good antibacterial adhesion and antibacterial growth performance, which are attributed to the synergistic effect of the superhydrophobicity and low adhesion on the surface, as well as the physical and chemical properties of AgNPs. The antibacterial properties of the PLP-S/AgNPs surface increased as immersion progressed. The anti-adhesion rates of PLP-S/$AgNPs_{12h}$ against *E. coli* and *S. aureus* were as high as 86.3% and 91.7%, respectively. In addition, the PLP-S/AgNPs samples effectively killed bacteria that adhered to the surface, thereby inhibiting the formation of bacterial biofilms. Therefore, this type of coating with superhydrophobic/antibacterial properties can potentially be applied to the surface of medical devices to improve and extend their antibacterial properties.

Acknowledgements

The authors gratefully acknowledge the National Natural Science Foundation of China (52175207) and the National Science and Technology Fund Project of China (2020-JCJQ-JJ-378).

Declaration of competing interest

The authors have no competing interests to declare that are relevant to the content of this article.

References

[1] An Y H, Friedman R J. Concise review of mechanisms of bacterial adhesion to biomaterial surfaces. *J Biomed Mater Res* **43**(3): 338–348 (1998)

[2] Zhang X X, Wang L, Levänen E. Superhydrophobic surfaces for the reduction of bacterial adhesion. *RSC Adv* **3**(30): 12003–12020 (2013)

[3] Feng L, Li S H, Li Y S, Li H J, Zhang L J, Zhai J, Song Y L, Liu B Q, Jiang L, Zhu D B. Super-hydrophobic surfaces: From natural to artificial. *Adv Mater* **14**(24): 1857–1860 (2002)

[4] Li J, Wei Y, Huang Z Y, Wang F P, Yan X Z, Wu Z L. Electrohydrodynamic behavior of water droplets on a horizontal super hydrophobic surface and its self-cleaning application. *Appl Surf Sci* **403**: 133–140 (2017)

[5] Zheng B Y, Kang J J, Di Y L, Wang H D, Zhu L N, Lan L. Study of the wettability of laser-built 3Cr13 stainless steel. *Surf Eng* **37**(12): 1484–1495 (2021)

[6] Zhang M, Wang P, Sun H Y, Wang Z K. Superhydrophobic surface with hierarchical architecture and bimetallic composition for enhanced antibacterial activity. *ACS Appl Mater Interfaces* **6**(24): 22108–22115 (2014)

[7] Di Y L, Qiu J H, Wang G, Wang H D, Lan L, Zheng B Y. Exploring contact angle hysteresis behavior of droplets on the surface microstructure. *Langmuir* **37**(23): 7078–7086 (2021)

[8] Aryanti P T P, Sianipar M, Zunita M, Wenten I G. Modified membrane with antibacterial properties. *Membr Water Treat* **8**(5): 463–481 (2017)

[9] Tavakolian M, Okshevsky M, van de Ven T G M, Tufenkji N. Developing antibacterial nanocrystalline cellulose using natural antibacterial agents. *ACS Appl Mater Interfaces* **10**(40): 33827–33838 (2018)

[10] Xi Y J, Song T, Tang S Y, Wang N S, Du J Z. Preparation and antibacterial mechanism insight of polypeptide-based micelles with excellent antibacterial activities. *Biomacromolecules* **17**(12): 3922–3930 (2016)

[11] Stankic S, Suman S, Haque F, Vidic J. Pure and multi metal oxide nanoparticles: Synthesis, antibacterial and cytotoxic properties. *J Nanobiotechnology* **14**(1): 73 (2016)

[12] Korkmaz N, Ceylan Y, Taslimi P, Karadağ A, Bülbül A S, Şen F. Biogenic nano silver: Synthesis, characterization, antibacterial, antibiofilms, and enzymatic activity. *Adv Powder Technol* **31**(7): 2942–2950 (2020)

[13] Liu H, Liu R, Ullah I, Zhang S Y, Sun Z Q, Ren L, Yang K. Rough surface of copper-bearing titanium alloy with multifunctions of osteogenic ability and antibacterial activity. *J Mater Sci Technol* **48**: 130–139 (2020)

[14] Sirelkhatim A, Mahmud S, Seeni A, Kaus N H M, Ann L C, Bakhori S K M, Hasan H, Mohamad D. Review on zinc oxide nanoparticles: Antibacterial activity and toxicity mechanism. *Nano Micro Lett* **7**(3): 219–242 (2015)

[15] Zhang W B, Wang S, Ge S H, Chen J L, Ji P. The relationship between substrate morphology and biological performances of nano-silver-loaded dopamine coatings on titanium surfaces. *Royal Soc Open Sci* **5**(4): 172310 (2018)

[16] Le Ouay B, Stellacci F. Antibacterial activity of silver nanoparticles: A surface science insight. *Nano Today* **10**(3): 339–354 (2015)

[17] Song L J, Sun L W, Zhao J, Wang X H, Yin J H, Luan S F, Ming W H. Synergistic superhydrophobic and photodynamic cotton textiles with remarkable antibacterial activities. *ACS Appl Bio Mater* **2**(7): 2756–2765 (2019)

[18] Qian H C, Li M L, Li Z, Lou Y T, Huang L Y, Zhang D W, Xu D K, Du C W, Lu L, Gao J. Mussel-inspired superhydrophobic surfaces with enhanced corrosion resistance and dual-action antibacterial properties. *Mater Sci Eng C* **80**: 566–577 (2017)

[19] Pan Q F, Cao Y, Xue W, Zhu D H, Liu W W. Picosecond laser-textured stainless steel superhydrophobic surface with an antibacterial adhesion property. *Langmuir* **35**(35): 11414–11421 (2019)

[20] Tian Y C, Jiao C C, Wang S, Cong H L, Shen Y Q, Yu B. Agar-based ZIF-90 antibacterial hydrogels for biomedical applications. *Ferroelectrics* **563**(1): 12–20 (2020)

[21] Liao Y, Wang Y Q, Feng X X, Wang W C, Xu F J, Zhang L Q. Antibacterial surfaces through dopamine functionalization and silver nanoparticle immobilization. *Mater Chem Phys* **121**(3): 534–540 (2010)

[22] Xie Y J, Yue L N, Zheng Y D, Zhao L, Liang C Y, He W, Liu Z W, Sun Y, Yang Y Y. The antibacterial stability of poly(dopamine) *in-situ* reduction and chelation nano-Ag based on bacterial cellulose network template. *Appl Surf Sci* **491**: 383–394 (2019)

[23] Liu Y L, Ai K L, Lu L H. Polydopamine and its derivative materials: Synthesis and promising applications in energy, environmental, and biomedical fields. *Chem Rev* **114**(9): 5057–5115 (2014)

[24] Lee H S, Scherer N F, Messersmith P B. Single-molecule mechanics of mussel adhesion. *PNAS* **103**(35): 12999–13003 (2006)

[25] Ball V, Nguyen I, Haupt M, Oehr C, Arnoult C, Toniazzo V, Ruch D. The reduction of Ag^+ in metallic silver on pseudomelanin films allows for antibacterial activity but does not imply unpaired electrons. *J Colloid Interface Sci* **364**(2): 359–365 (2011)

[26] Lee H A, Park E S, Lee H S. Polydopamine and its derivative surface chemistry in material science: A focused review for studies at KAIST. *Adv Mater* **32**(35): 1907505 (2020)

[27] Zheng X Y, Zhang J X, Wang J, Qi X Q, Rosenholm J M, Cai K Y. Polydopamine coatings in confined nanopore space: Toward improved retention and release of hydrophilic cargo. *J Phys Chem C* **119**(43): 24512–24521 (2015)

[28] Wenzel R N. Resistance of solid surfaces to wetting by water. *Ind Eng Chem* **28**(8): 988–994 (1936)

[29] Cassie A B D, Baxter S. Wettability of porous surfaces. *Trans Faraday Soc* **40**: 546–551 (1944)

[30] Qing Y A, Cheng L, Li R Y, Liu G C, Zhang Y B, Tang X F, Wang J C, Liu H, Qin Y G. Potential antibacterial mechanism of silver nanoparticles and the optimization of orthopedic implants by advanced modification technologies. *Int J Nanomed* **13**: 3311–3327 (2018)

[31] Li W R, Xie X B, Shi Q S, Zeng H Y, Ou-Yang Y S, Chen Y B. Antibacterial activity and mechanism of silver nanoparticles on *Escherichia coli*. *Appl Microbiol Biotechnol* **85**(4): 1115–1122 (2010)

[32] Klueh U, Wagner V, Kelly S, Johnson A, Bryers J D. Efficacy of silver-coated fabric to prevent bacterial colonization and subsequent device-based biofilm formation. *J Biomed Mater Res* **53**(6): 621–631 (2000)

[33] Hamad A, Khashan K S, Hadi A. Silver nanoparticles and silver ions as potential antibacterial agents. *J Inorg Organomet Polym Mater* **30**(12): 4811–4828 (2020)

Ling LAN. He is currently pursuing a master degree at China University of Geosciences (Beijing). His main research areas are superhydrophobic materials.

Yue-lan DI. She received her Ph.D. degree in material science and engineering from Academy of Army Armored Forces, China, in 2013 and joined National Defense Key Laboratory of Equipment Remanufacturing Technology, China, from 2014. Her research areas cover the design of structure-function integrated coatings and surface interface friction characteristics.

Hai-dou WANG. He received his Ph.D. degree in the Department of Mechanical Engineering from Tsinghua University, China, in 2003. He joined the National Key Laboratory for Remanufacturing at Academy of Army Armored Forces, China, from then on. He is now a professor and the deputy director of the laboratory. His current research areas cover surface engineering, remanufacturing, and tribology, especially in service life evaluation of surface coatings and solid film lubrication.